OPTICAL TECHNIQUES FOR MEASURING NANOPARTICLE LOADING AND DISPERSION

W. R. Broughton[1*], T. Koukoulas[1], M. Tedaldi[1], P. D. Theobald[1]

[1]*National Physical Laboratory, Teddington, Middlesex, TW11 0LW, United Kingdom*
**bill.broughton@npl.co.uk*

Keywords: Polymeric nanocomposites, optical characterization, dispersion.

Abstract
This paper presents three non-invasive optical and image processing techniques; frequency-domain optical coherence tomography (FD-OCT), Fraunhofer wavefront correlation (FWC) and oscillatory photon correlation spectroscopy (Os-PCS), for discriminating between different particle loadings and levels of dispersion. The three techniques, based on optical diffraction and diffusion mechanisms have been applied to a range of polymeric nanocomposites (PNCs) including nanoclay reinforced epoxy, zinc oxide and lithium aluminate reinforced polypropylene, and multi-walled carbon nanotube (MWCNT) reinforced epoxy with different levels of particle loading and dispersion.

1 Introduction

The inclusion of small concentrations of nanoparticles in polymers (typically <5 wt. %) can enhance mechanical and physical properties of polymer nanocomposites (PNCs). Dispersion of nanoparticles during mixing is problematic with poor mixing resulting in particle agglomeration (i.e. particle clustering), which subsequently limits the potential for property enhancement. A general consensus is that achieving good dispersion is a key step towards large-scale production and commercialization of PNCs, and that a reliable in-situ measurement technique for production and in-service inspection capable of quantitatively characterizing particle loading and dispersion would significantly assist in fulfilling the potential of PNCs. A variety of techniques, such as X-ray diffraction (XRD), transmission electron microscopy (TEM), dielectrics and rheological characterization, ultrasonic resonance spectroscopy, scanning acoustic microscopy, laser-ultrasound, infrared spectroscopy, Raman spectroscopy and light transmission have been considered in an attempt to characterize particulate properties, such as size/shape (and distributions) and dispersion [1-2]. XRD can provide a wealth of information on the structural, physical and chemical nature of materials [3-4]. It is often used for characterizing the structure of PNCs, providing detailed information on the extent of intercalation (e.g. interlayer spacing d_{001}) and exfoliation of particulates. The positions and shapes of the peaks obtained from angular dependent intensity plots can provide information on the structure of the diffracting species and in some cases the degree of dispersion [3]. However, the results are difficult to interpret due to factors such as peak broadening, resulting from the superposition of multiple peaks from incomplete intercalation or complete loss of signal due to extremely poor dispersion [4].

TEM is an immensely powerful although destructive technique, capable of providing high-resolution images at the nanoscale. The miniscule sample quantities (10^{-18} kg) required for TEM imaging are not representative of the bulk material, and hence a large number of images are required in order to provide sufficient information on levels of loading and dispersion. Moreover, the structure of the material, and hence its physical properties, may alter as a result of the preparation process.

The ability of the above-mentioned techniques to discriminate between different levels of loading and dispersion is very limited. The techniques often require special sample preparation (destructive in most cases), involve the analysis of extremely small sample areas and long measurement times, and quite often produce ambiguous results that are difficult to evaluate and interpret. Instrumentation and preparation costs are also often prohibitive. The research work presented here demonstrates the potential of utilizing frequency-domain optical coherence tomography (FD-OCT), Fraunhofer wavefront correlation (FWC) and oscillatory photon correlation spectroscopy (Os-PCS) for discriminating between different levels of particle loading and dispersion. The first two techniques are essentially static light scattering techniques while the third involves dynamic light scattering. Crucial parameters in this case are not only the successful discrimination of materials based on their loading and dispersion profiles, but also the possibility of measuring and analyzing large material areas compared to the standard techniques listed above, in addition to being non-destructive, fast and suitable for in-line inspection.

2 Materials

Four different PNC systems classified as Materials 1, 2, 3 and 4 (listed below) have been investigated using the three optical techniques.

Material 1: Organoclay Nanomer® 1.30E, an octadeylamine modified montmorillonite, reinforced Huntsman LY 564 epoxy resin with Ardur 2954 hardener with varying particle loading and dispersion profiles. The materials, listed in Table 1, were supplied by BAe Systems (Operations) Ltd in the form of 3 mm thick autoclave cured plaques with varying degrees of particle loading and dispersion. The autoclave cure cycle consisted of an initial temperature ramp to 80 °C at 4 °C/min, dwell of 1 hour at 80 °C followed by cooling to room temperature (15-18 hrs). Pressure was ramped to ~80 psi at 14 psi/min at the start of the cure cycle. The plaques were post-cured at 140 °C for 8 hrs. Average planar dimensions of the nanoclay particles (platelets) were 0.74 ± 0.34 mm and 0.51 ± 0.22 mm, respectively. Intra-gallery (d_{001}) spacing is 1.8-2.2 nm (Nanocor technical datasheet for Nanomer® 1.30 E).

Material 2: Zinc oxide (ZnO) particulate reinforced polypropylene (PP) with varying particle loading (0.0 wt. %, 2.0 wt. %, 5.0 wt. % and 10.0 wt. %). The materials supplied by University of Brunel. The materials were supplied as 1 mm thick panels.

Material 3: Lithium aluminate ($LiAlO_2$) reinforced PP with 2.0 wt. % particle loading and three different mixing times (untreated, 1 and 2 hours) supplied by University of Brunel.

Material 4: C150P Bayertubes® multi-walled carbon nanotube (MWCNT) reinforced Gurit modified di-glycidyl ether of bisphenol F (DGEBF) epoxy resin. The PNC materials with varying particle loading (0 to 1.5 wt. %) were supplied as 25 mm square sections ~2-3 mm thick by the Advanced Composites Centre for Innovation and Science (University of Bristol).

Material	Density [kg/cm^3]	Weight Fraction [%]	Volume Fraction [%]
Neat resin	1.1328 ± 0.0006	0.00	0.00
1.0 wt. %			
Poor	1.1400 ± 0.0008	1.04 ± 0.01	0.94 ± 0.10
Moderate	1.1412 ± 0.0007	1.06 ± 0.01	1.10 ± 0.10
Good	1.1398 ± 0.0008	1.04 ± 0.03	0.91 ± 0.11
2.0 wt. %			
Good	1.1449 ± 0.0002	2.03 ± 0.01	1.57 ± 0.03
4.0 wt. %			
Poor	1.1579 ± 0.0003	4.13 ± 0.01	3.27 ± 0.04
Good	1.1560 ± 0.0005	3.89 ± 0.10	3.03 ± 0.06

Table 1. Density, weight fraction and volume fraction of the nanoclay/epoxy materials.

Note: It needs to be emphasized that whilst current manufacturing practices specify particle loading as a numerical value, the level of dispersion is provided only as a description (i.e. qualitative or subjective assessment).

Table 2 shows the density of the ZnO/PP, $LiAlO_2$/PP and MWCNT/epoxy materials investigated in the study.

Material	Density [kg/cm^3]
ZnO/PP	
Neat resin	0.8986
2.0 %	0.9011
5.0 %	0.9092
10.0 %	0.9216
$LiAlO_2$/PP	
Untreated	0.8961
1 hour mixing	0.9053
2 hour mixing	0.9040
MWCNT/Epoxy	
Neat resin	1.1450
0.5 %	1.1521
1.0 %	1.1500
1.5 %	1.1495

Table 2. Density of ZnO/PP, $LiAlO_2$/PP and MWCNT/epoxy materials.

3 Optical techniques

3.1 Fourier domain - optical coherence tomography (FD-OCT)

OCT is based on low coherence interferometry (LCI) and works to a depth of ~ 2-3 mm with the depth of penetration decreasing with increasing particle loading. The dominant contrast mechanism utilized in LCI is variation in refractive index that gives rise to an increase in direct backscattering of incoming photons [5]. By inverse Fourier transformation of the resulting back-scattered radiation, it is possible to acquire two-dimensional (2-D) information resulting from refractive index boundaries within the material [5]. The resulting visual data represents information from adjacent depth layers that can be stacked together to provide a three dimensional (3-D) representation. A distinct difference in refractive index exists between the nanoparticles, which act as light scatterers, and the surrounding polymer matrix.

In this case, FD-OCT was utilized; a Michelson Diagnostics EX1301 multi-beam OCT microscope was used; operating in a swept frequency mode with a wavelength of 1305 nm (infrared) and bandwidth of 150 nm. The system consists of four laser beams focused at different depths over a depth of focus of 0.25 mm each, providing a total focal range of 1 mm. Although nanoparticles may be few nanometres in diameter or thickness (e.g. nanoclay platelets and MWCNTs), particle lengths are often a few microns, which is of sufficient magnitude to interact with the interrogating laser beam. The tomographic method provides a highly sensitive measurement tool that can accurately map the sample at different depths even if the refractive index difference between the polymer itself and the nanoparticles is small.

In order to numerically quantify the visual representation resulting from the measurement data, it is necessary to post-process the images. Each of the acquired images is firstly decomposed into their horizontal, vertical and diagonal wavelets. Each wavelet dimension is then divided into a 2-D segment array and the standard deviation of the image per segment is calculated. The overall standard deviation of that layer gives therefore an indication of its texture; higher deviation effectively means lower level of uniformity (see Figure 1). Each layer is also analyzed in terms of particle count and total area covered. By repeating the process throughout the material, an accurate picture of the level of dispersion can be provided.

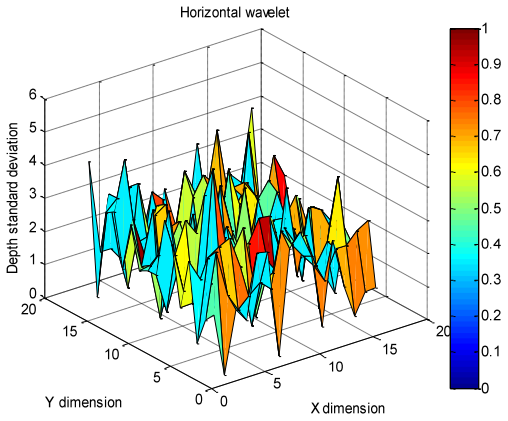

Figure 1. Horizontal wavelet for 1.0 wt. % MWCNT/epoxy.

3.2 Fraunhofer wave correlation (FWC)

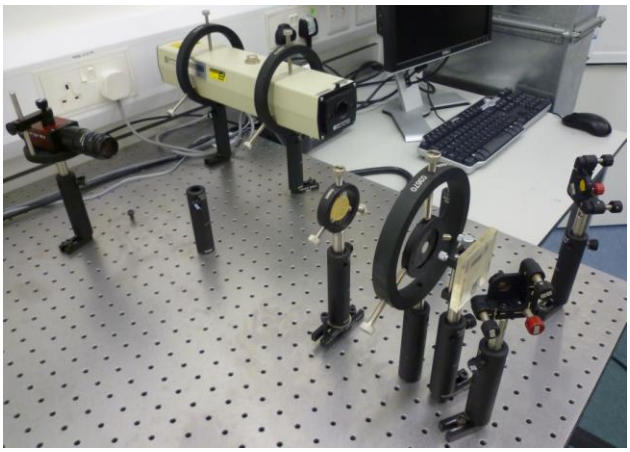

Figure 2. Fraunhofer wave correlation (FWC) set-up.

In this case, coherent light from a He:Ne low power laser source (1 mW) with a wavelength of 633 nm is directed onto a diffraction grating that produces a 2-D pattern of dots; this optical wavefront is captured by a CCD camera placed at an angle to the axis of propagation in order to avoid the zero-order component of the laser light (see Figure 2). The level of dispersion and particle loading in a PNC effectively produces a physical medium that will directly affect the optical properties of the 2-D optical wavefront. A material with no fillers (neat resin) will produce very little diffusion of the optical pattern since the refractive index is almost identical per unit area (uniform); however the level of diffusion will change for different levels of particle loading and dispersion. Emerging optical wavefronts can subsequently be captured and analyzed in order to produce discrimination metrics.

The analysis is based on frequency-based cross-correlation of the captured images. The wavefront from the neat resin may be represented as a spatial reference function, while those from PNCs represent input functions. Figure 3 shows typical FWC data obtained for nanoclay epoxy samples: cross-correlation between the reference (i.e. epoxy with no platelets) and 1 wt. % good dispersion (left) and 4 wt. % poor dispersion (right). In each case, the spectrum of each function is calculated, a fully complex multiplication is performed between reference and input and the result is inverse Fourier transformed to yield the correlation function as a 2-D plane. Within that plane, the signal region is defined as the area around the DC component, while the noise region is the rest of the plane. By applying an iterative low-pass spatial filter on the spectra prior to the fully complex multiplication it is possible to calculate the signal-to-noise ratio (SNR) relating to the level of spatial high frequencies rejected by the algorithm. The standard deviation between the SNR from all iteration stages is then calculated and its value assigned to the specific material.

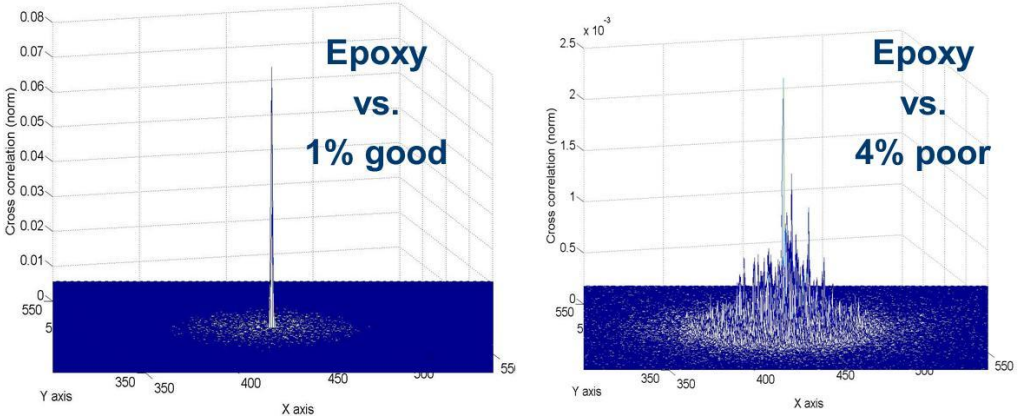

Figure 3. FWC (correlation plane) energies for nanoclay/epoxy samples.

3.3 Oscillatory photon correlation spectroscopy (Os-PCS)

In generic terms, photon correlation spectroscopy is mostly applicable to the measurement of specific properties of fluids. It often utilizes two laser beams that are crossed to form an ellipsoid with interference fringes within the medium under investigation (see Figure 4). Scattered photons from the interference region are collected and a photo-multiplier tube produces photon pulse sequences that are correlated by suitable hardware in order to yield specific meausurands relating to the medium.

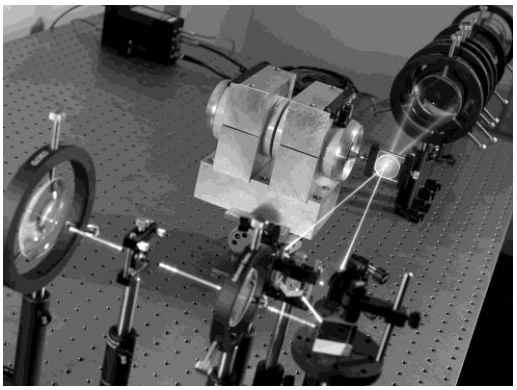

Figure 4. Oscillatory-photon correlation spectroscopy (Os-PCS) experimental set-up.

For this study, samples were oscillated at specific amplitudes and frequencies (depending on the spatial resolution required) within the interference region so that the process becomes dynamic. The scattered photon radiation was analyzed in order to produce the so-called auto-correlation function (ACF); this effectively is the correlation between a photon sequence and its delayed version. In this case, the dynamic range of the ACF is analyzed. A single mode, frequency, doubled, Nd:YAG laser source (532 nm wavelength) was used. Uniform levels of dispersion effectively produce a material that is highly homogeneous. This results in a uniform number of photons been scattered per unit area, thus producing ACFs of high dynamic range. As the level of loading increases, the dynamic range decreases accordingly. Moderate and poor levels of dispersion will reduce the homogeneity within the material, thus reducing the ACF dynamic range. By calculating the logarithmic trend-line of each ACF and plotting all functions, it is possible to decouple the particle loading from the dispersion level.

4 Experimental results

4.1 Nanoclay reinforced epoxy

The results in Tables 3 and 4 clearly show differences between the nanoclay/epoxy materials, demonstrating the ability of all three techniques to differentiate between the various levels of particle loading and dispersion (see also Figure 5). The trends shown in Tables 3 and 4 are dependent on the wavefront-particle interaction involved. ACF dynamic range decreases with increasing particle loading and decreasing particle uniformity. Os-PCS photon count and FWC multiple-bandwidth difference responses are the converse of ACF. OCT standard deviation and FWC greyscale values decrease with increasing particle loading, and increase as the dispersion profile (non-uniformity) worsens.

Material	**FWC**		**Os-PCS**	
	Greyscale (mean)	**Multiple-Bandwidth Difference (Standard Deviation)**	**Photon Count (mean, × 10^6)**	**ACF Dynamic Ranges (mean, × 10^{-5})**
1.0 wt. %				
Poor	105	0.39926	11.84	3.18
Moderate	101	0.36700	11.08	3.89
Good	91	0.03348	8.08	6.88
2.0 wt. %				
Good	87	0.10444	9.47	5.67
4 0 wt. %				
Poor	80	0.44577	13.48	2.59
Good	77	0.10432	10.45	4.73

Table 3. FWC and Os-PCS optical data for the nanoclay/epoxy materials.

Material	Standard Deviation
1.0 wt. %	
Poor	4.276
Moderate	3.879
Good	3.681
2.0 wt. %	
Good	3.454
4.0 wt. %	
Poor	3.173
Good	2.944

Table 4. OCT mean standard deviation data for MWCNT/epoxy materials – see also [6].

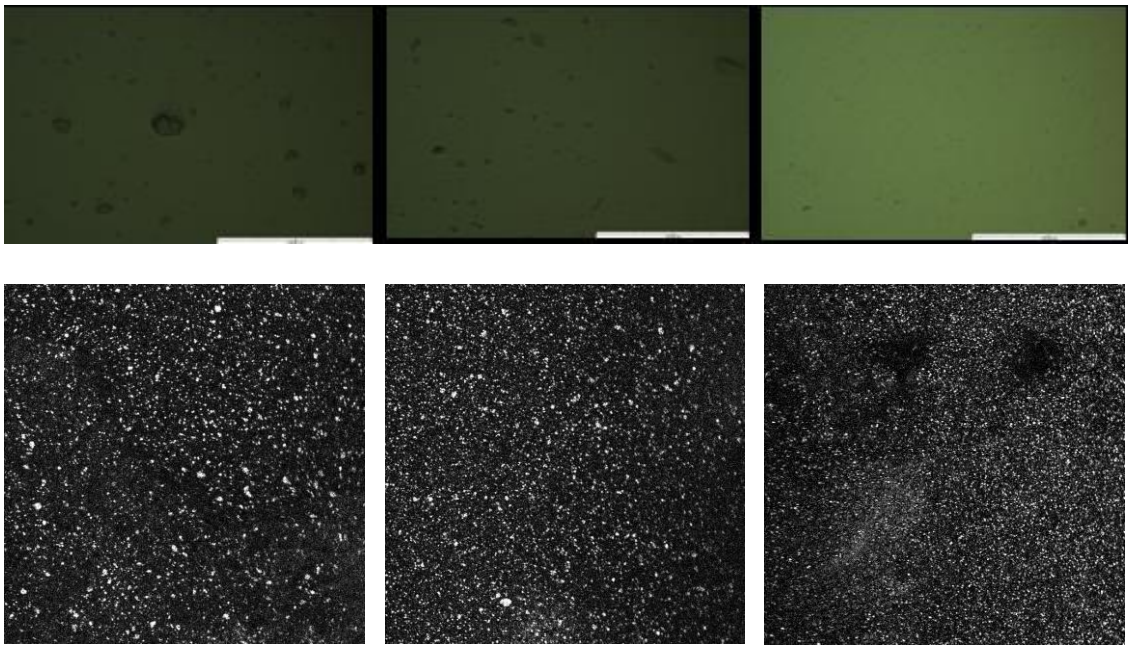

Figure 5. Optical micrographs - 250 µm scale bar (top) and 3 mm × 3 mm OCT images (bottom) of 1.0 wt. % nanoclay/epoxy with poor dispersion (left), moderate dispersion (centre) and good dispersion (right).

4.2 Zinc oxide and lithium aluminate

ZnO and $LiAlO_2$ were interrogated using both FWC and FD-OCT. Table 5 compares the results obtained using the two techniques. The laser beam in both cases was able to penetrate the two semi-transparent materials and provide key information relating to particle loading and dispersion. The lithium aluminate results indicate that increasing mixing times improves particle uniformity, although the changes are relatively modest.

Material	OCT	FWC
ZnO/PP		
Neat resin	1.93	Not applicable
2.0 wt. %	2.01	9.838
5.0 wt. %	2.10	8.626
10.0 wt. %	2.15	7.175
$LiALO_2$/PP		
Untreated	2.21	11.801
1 hour mixing	2.38	9.087
2 hour mixing	2.45	8.933

Table 5. Mean OCT and FWC standard deviation values for ZnO/PP and $LiAlO_2$/PP materials.

4.3 MWCNT reinforced epoxy

In order to examine the MWCNT/epoxy materials it is necessary to operate in the infra-red portion of the spectrum, hence only FD-OCT and Os-PCS are suitable for these materials. OCT was able to penetrate to ~250 μm in depth, sufficient to detect differences in particle loading and dispersion profiles (see Table 6). In order to minimize the effects of surface artefacts and multiple reflections, analysis was also carried out on a single layer located at a depth of 20 μm (Layer-5) from the surface (see Table 6).

Material	OCT	
	Volumetric	Layer-5
Neat resin	1.35	28.68
0.5 %	2.30	26.82
1.0 %	1.96	26.34
1.5 %	2.08	24.74

Table 6. OCT mean standard deviation data for MWCNT/epoxy materials.

5 Conclusions

Using the different techniques it is possible to provide a quantitative assessment of particle loading and dispersion profile as demonstrated by the FD-OCT, FWC and Os-PCS data presented in this paper. There is a caveat and that being the limit at which these techniques can operate. Sensitivity limitations exist relating to the minimum particle size that will interact with the laser beam (dependent on wavelength) and refractive index boundary differences between the optical scatterers and the surrounding matrix. Signal saturation is another issue; limiting the maximum particle loading that can be interrogated. Optical properties can differ significantly between composite systems, which needs to be considered when analyzing the optical data (no one size fits all).

Acknowledgements

The authors acknowledge the financial support provided by United Kingdom Department for Business, Innovation and Skills (National Measurement Office), as part of the Materials 2010 Programme. The authors would also like to thank Amir Rezai (BAe Systems (Operations) Ltd), Karnik Taverdi (University of Brunel), and Sameer Rahatekar and John Williams (Advanced Composites Centre for Innovation and Science (ACCIS) - University of Bristol) for their technical support and advice.

References

[1] Broughton, W.R. Characterisation of Nanosized Filler Particles in Polymeric Systems: A Review, *National Physical Laboratory Report Mat 12*, National Physical laboratory, Teddington, UK (2008).

[2] Utracki, L.A. Clay-Containing Polymeric Nanocomposites, **Volume 1**, Rapra Technology Limited, Shawbury, United Kingdom (2004).

[3] Mai, Y.-W., Yu, Z.-Z. Clay-Acrylate Nanocomposite Photopolymers, **Chapter 7**, Woodhead Publishing Limited, Oxford, United Kingdom (2006).

[4] Decker, C., Keller, L., Zahouily, K., Benfarhi, S. Synthesis of Nanocomposite Polymers by UV-Radiation Curing, *Polymer*, **Volume 46**, pp. 6640-6648 (2005).

[5] Schmitt, J.M. Optical Coherence Tomography (OCT): A Review, *IEEE Journal of Selected Topics in Quantum Electronics*, **Volume 5**, pp. 1205-1215 (1999).

[6] Koukoulas, T., Broughton, W.R., Theobald, P.D., Tedaldi, M. Characterization of Solid Complex Multiphase Systems Based on Oscillatory Photon Correlation Spectroscopy, *Optics Letters*, **Volume 35(22)**, pp. 3754-3756 (2010).